scientific reports

Check for updates

OPEN

MgO-enhanced β-TCP promotes osteogenesis in both in vitro and in vivo rat models

Kenichiro Saito[1], Yusuke Inagaki[2]✉, Yoshinobu Uchihara[1], Masakazu Okamoto[1], Yuki Nishimura[1], Akihito Kawai[1], Tatsuro Sugino[3], Kensuke Okamura[1], Munehiro Ogawa[4], Akira Kido[2] & Yasuhito Tanaka[1]

Allogeneic bone grafts are used to treat bone defects in orthopedic surgery, but the osteogenic potential of artificial bones remains a challenge. In this study, we developed a β-tricalcium phosphate (β-TCP) formulation containing MgO, ZnO, SrO, and SiO_2 and compared its bone-forming ability with that of β-TCP without biological elements. We prepared β-TCP discs with 60% porosity containing 1.0 wt% of these biological elements. β-TCP scaffolds were loaded with bone marrow-derived mesenchymal stem cells (BMSC) from 7-week-old male rats and cultured for 2 weeks. ALP activity and mRNA expression of osteogenic markers were evaluated. In addition, scaffolds were implanted subcutaneously in rats and analyzed after 7 weeks. In vitro, the MgO group showed lower Ca concentrations and higher osteogenic marker expression compared to controls. In vivo, the MgO group showed higher ALP activity compared to controls, and RT-qPCR analysis showed significant expression of *BMP2* and *VEGF*. Histopathology, fluorescent immunostaining, and micro-CT also showed relatively better bone formation in the MgO group. β-TCP with MgO may enhance bone morphology in vitro and in vivo and improve the prognosis of patients with substantial and refractory bone defects.

Keywords Allogeneic bone grafts, β-tricalcium phosphate, Bone marrow-derived mesenchymal stem cells osteogenesis

Orthopedic surgeons have historically resorted to allogeneic bone grafts to address bone defects from traumatic injuries or bone malignancies. However, the constraints imposed by limited graft size and invasive procedures have presented formidable challenges. Consequently, instead of allogeneic, synthetic ceramic artificial bones and polymeric biomaterials have been clinically applied and are undergoing further development. Notable polymer-based biomaterials are polyether–ether–ketone (PEEK) and polyethylene terephthalate (PET). Calcium phosphate (CaP) ceramics have emerged as a paragon of biocompatible biomaterials among synthetic ceramic substitutes. Among such materials, hydroxyapatite and β-tricalcium phosphate (β-TCP) are considered prototypical artificial bones. β-TCP formulations exhibit high bio-absorption but modest osteo-conductivity, rendering them relatively less effective in terms of their osteogenic potential compared to their homologous bone counterparts.

Consequently, enhancing the ability of β-TCP formulations to promote bone growth remains a challenge[1,2].

One effective strategy to boost the bone-promoting potential of β-TCP formulations is to incorporate small amounts of biological elements found in living organisms into artificial bones. These bio-elements include zinc (Zn) and silicon (Si). Zn is an essential trace element that has been shown to promote bone formation both in vitro and in vivo. Si is also an important trace element that promotes bone formation and calcification. In vitro studies have reported that Zn has a specific stimulating effect on osteoblasts and a strong inhibitory effect on bone resorption caused by osteoclasts[3–5]. An in vivo study using rabbit femurs demonstrated that Zn-doped CaP formulations led to an increase of over 50% in newly formed bone compared to undoped CaP formulations[6]. Similarly, in vitro studies suggest that adding up to 9.0 wt% of silicon dioxide (SiO_2) can promote osteoblast differentiation, indicating a high bone-promoting potential. Therefore, both in vitro and in vivo results indicate that CaP formulations incorporating these bio-elements can enhance bone formation and biological responses. However, the mechanisms and cellular events involved in bone growth mediated by these additives are still unclear[7–9].

[1]Department of Orthopedic Surgery, Nara Medical University, Kashihara, Nara, Japan. [2]Department of Rehabilitation Medicine, Nara Medical University, Kashihara, Nara, Japan. [3]Product Development Department, Olympus Terumo Biomaterials Corp., Shizuoka, Japan. [4]Department of Sports Medicine, Nara Medical University, Kashihara, Nara, Japan. ✉email: yinagaki@naramed-u.ac.jp

Previously, we reported the osteogenic differentiation of bone marrow-derived mesenchymal stem cells (BMSCs) on PEEK, PET, and β-TCP coated with a blend of bio-trace elements, including Zn, strontium (Sr), and Si. We elucidated their discrete potential to elicit osteogenic propensity[10–12]. In this context, magnesium (Mg), a biological element distinct from Zn, Sr, and Si, in β-TCPs has aroused substantial interest. Renowned for its multifaceted biological roles, Mg is essential for many cellular processes, notably impacting bone formation and metabolism[13]. Moreover, the characteristics of Mg, specifically its low density, commendable biocompatibility, and elastic modulus approximating that of normal bone tissues, accentuate its appeal[14,15]. Previous studies suggest its involvement in qualitative changes in the bone matrix, indirectly affecting mineral metabolism, promoting catalytic reactions, and regulating biological functions[16].

In this study, we prepared β-TCP formulations containing MgO, Zn oxide (ZnO), Sr oxide (SrO), and SiO_2 and compared these β-TCP formulations with element-free β-TCP formulations (control) using BMSCs. We aimed to investigate the impact of incorporating these biologically active elements into β-TCP formulations on enhancing osteogenic potential.

Results

In vitro studies

Calcium concentrations in culture supernatants

On day 14, the MgO group had significantly lower Ca concentrations in culture supernatants than the control group ($P < 0.05$). No significant differences were observed in the other groups when compared with the control group ($P > 0.05$) (Fig. 1).

Assessment of ALP activity

The MgO group exhibited significantly higher ALP activity than the control group ($P < 0.05$). No significant differences were observed in the other groups when compared with the control group ($P > 0.05$) (Fig. 2).

RT-qPCR analyses

Considering the mRNA expression levels of alkaline phosphatase (*ALP*), bone morphogenetic protein 2 (*BMP-2*), collagen type I alpha 1 (*COL1A1*), runt-related transcription factor 2 (*RUNX2*), osteocalcin (*OC*), and vascular endothelial growth factor (*VEGF*) genes, the MgO group displayed significantly higher levels than the control group ($P < 0.05$). No significant differences were observed in the other groups when compared with the control group ($P > 0.05$) (Fig. 3).

In vivo studies

Assessment of ALP activity

The MgO group had significantly higher ALP activity than the control group ($P < 0.05$) (Fig. 4).

RT-qPCR analyses

No significant differences were observed between the MgO and control groups in terms of mRNA expression levels of *BMP-2* and *VEGF* genes ($P < 0.05$) (Fig. 5).

Histological analyses

Seven weeks post-implantation, the β-TCP discs that were implanted subcutaneously were collected and stained with hematoxylin and eosin. Histological examination revealed that the MgO group exhibited superior bone

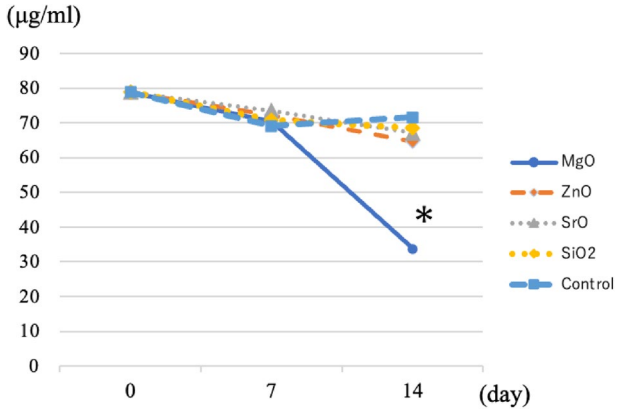

Fig. 1. Calcium concentration in nano-coated PET fiber artificial ligament culture medium. Calcium concentration on the 7th and 14th day was recorded. Calcium concentration in MgO was significantly lower than in ZnO, SrO, SiO_2 and the non-coated sample on the 14th day of the culture supernatant. The solid and broken lines indicate the data obtained in MgO, ZnO, SrO, SiO_2 and non-coated samples. Data are shown as the mean ± SD. Asterisk indicates $P < 0.05$ versus non-coated group (control).

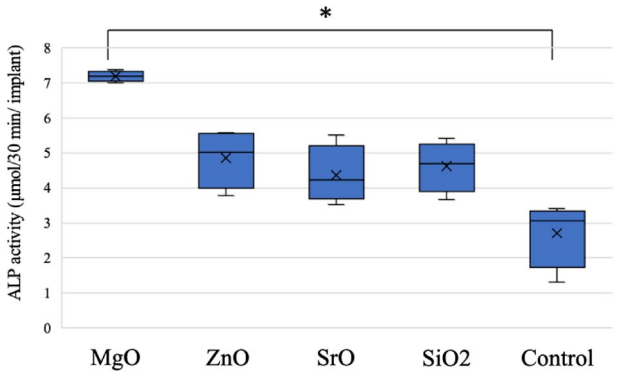

Fig. 2. Biochemical evaluation of each β-TCP group after osteogenic culture for 14 days. ALP activity is significantly higher in MgO than in ZnO, SrO, SiO2 and controls. Values are shown as means ± standard deviation. (n = 4 *$P < 0.05$.)

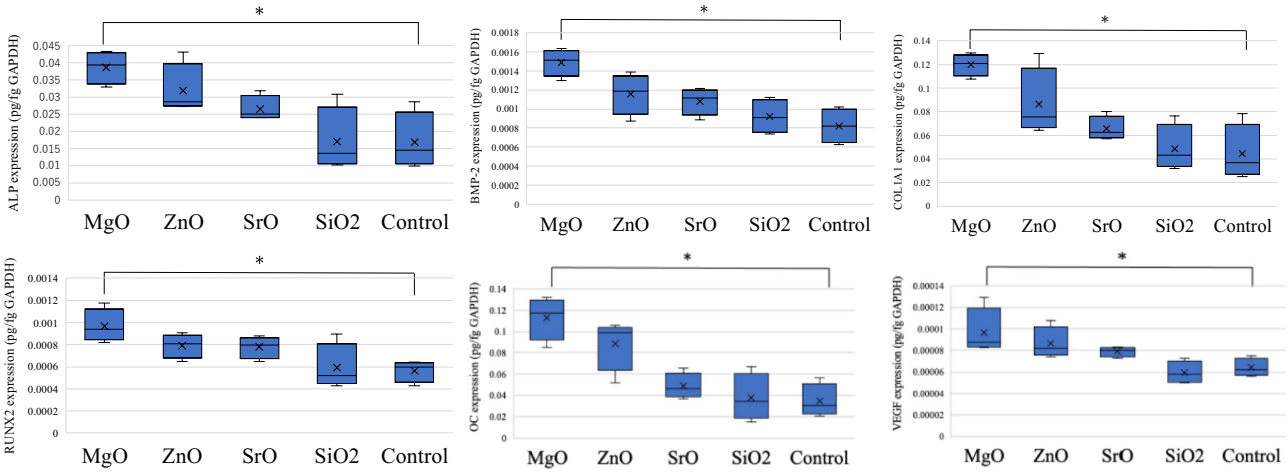

Fig. 3. mRNA expression levels in each group after osteogenic culture for 14 days, as evaluated by qRT-PCR. Values are shown as means ± SD (n = 5). *$P < 0.05$.

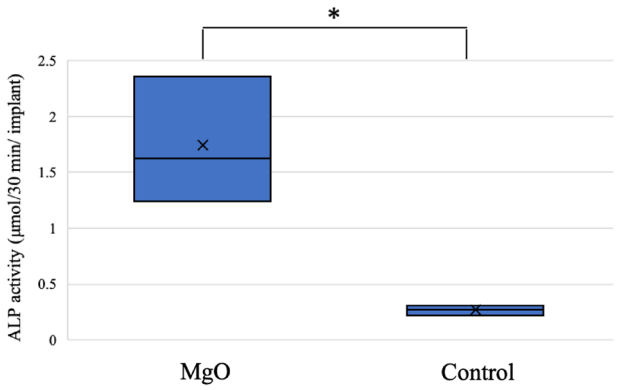

Fig. 4. Biochemical evaluation of each β-TCP group harvested 7 weeks after implantation. ALP activity is significantly higher in MgO than in controls. Values are shown as means ± standard deviation. (n = 3). *$P < 0.05$.

formation compared to the control group, indicating a relatively higher bone-forming capacity in the MgO group (Fig. 6).

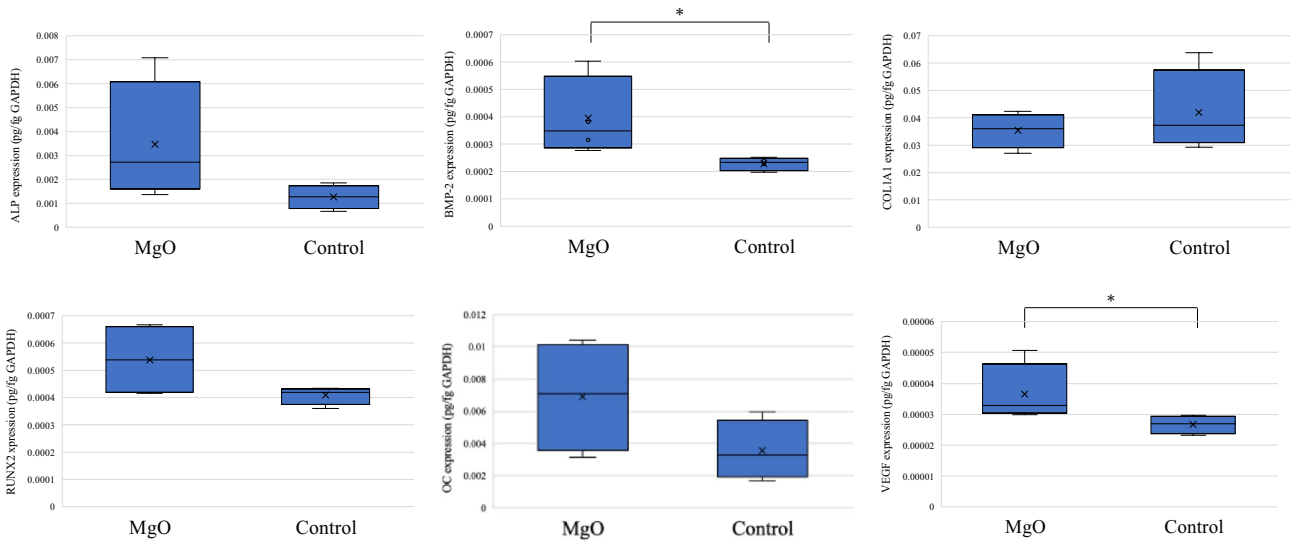

Fig. 5. mRNA expression levels in each group harvested 7 weeks after implantation, as evaluated by qRT-PCR. Values are shown as means ± SD (n = 4). *$P < 0.05$.

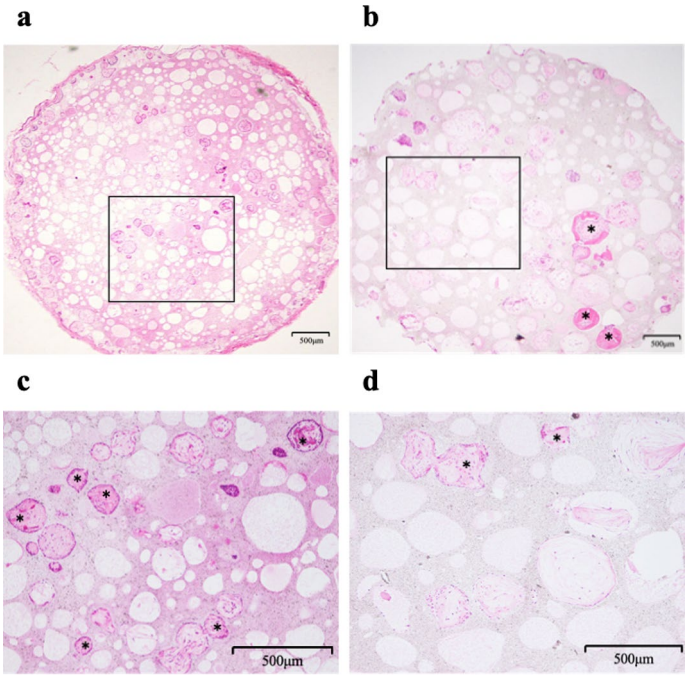

Fig. 6. Histological analysis of β-TCP harvested 7 weeks after implantation. HE staining shows more bone formation in MgO than in controls. (**a**), MgO; (**b**), control. (**c**, **d**) Higher magnifications of boxes indicated in (**a**) and (**b**), respectively. *Bone tissue.

Immunofluorescence staining

Seven weeks after implantation, the subcutaneously implanted β-TCP discs were harvested and subjected to fluorescence immunostaining with an antibody for type I collagen. The MgO group stained better in the bone than the control group and showed superior bone formation, indicating the relatively higher bone-forming capacity of the MgO group (Fig. 7).

Micro-computed tomography (micro-CT) analysis

Seven weeks post-implantation, bone formation was observed in both groups. The MgO group exhibited greater bone formation than the control group in the internal part of the artificial bone porosity (Fig. 8).

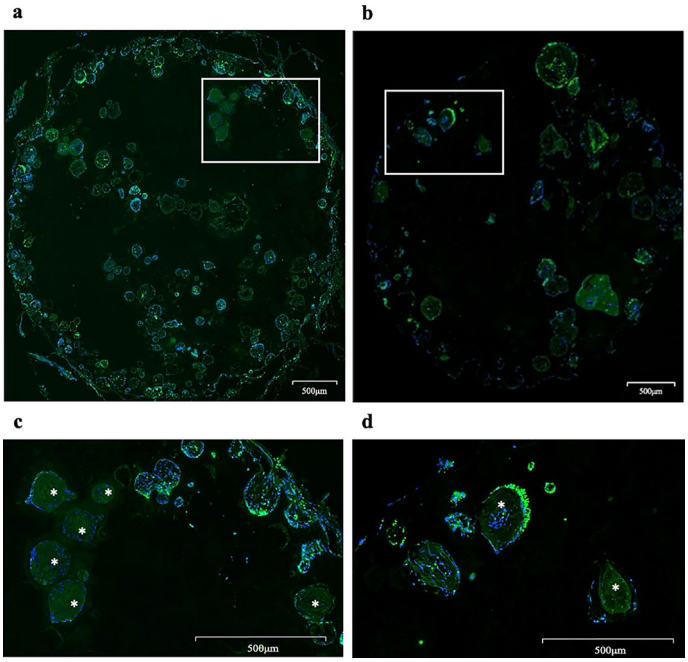

Fig. 7. Immunofluorescence Staining of β-TCP harvested 7 weeks after implantation. Collagen 1 staining shows more bone formation in MgO than in controls. (**a**), MgO; (**b**), control. (**c**, **d**) Higher magnifications of boxes indicated in (**a**) and (**b**), respectively. *Bone tissue.

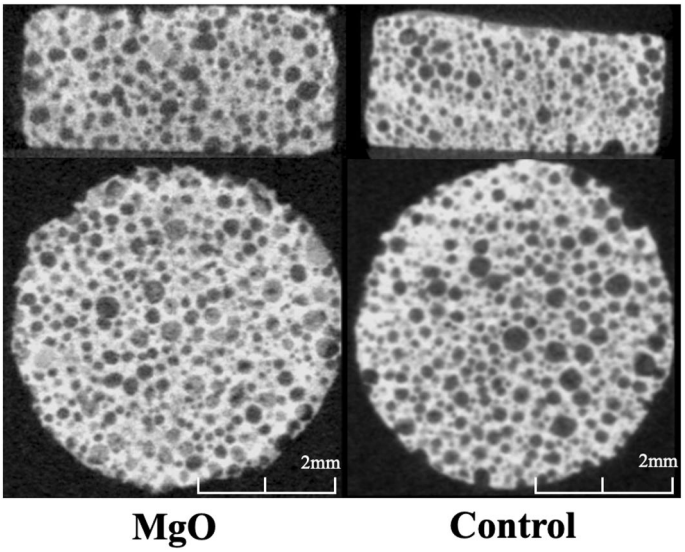

Fig. 8. Micro-CT analysis of β-TCP harvested 7 weeks after implantation. Representative images of two samples; MgO and Control.

Discussion

The clinical application of β-TCP formulations as a bone replacement material is severely limited owing to its poor osteoinductive capacity and insufficient bone formation. One prominent strategy that could augment the osteoinductive capacity of β-TCP formulations involves incorporating biological elements well-known for their pivotal roles in bone development, growth, and repair. This approach is of considerable interest owing to its superior safety profile and limited adverse effects. Notably, the inclusion of these biological elements within bone replacement materials can stimulate new bone generation in vivo[9,17], inhibit material degradation, and improve mechanical strength[18,19].

Among these biological elements, Mg holds prominence, as it is indispensable for various cellular processes and plays a crucial role in osteogenesis and metabolism[13]. Mg deficiency detrimentally impacts all stages of bone metabolism, precipitating arrested bone growth, diminishing osteoblastic and osteoclastic activities, and causing

osteopenia and heightened bone fragility[20,21]. Recently, it was reported that specific concentrations of Mg^{2+} ions play a pivotal role in new bone formation and bone regeneration. Adding Mg^{2+} ions may be a simple and effective way of promoting osteogenesis and angiogenesis in bio-ceramic scaffolds and improving the evolution of biomaterials for bone tissue engineering scaffolds[22]. Furthermore, the positive impact of Mg extends to fostering matrix mineralization and elevating collagen type X expression in mesenchymal stem cells[23]. Additionally, Mg propels osteoblast differentiation, enhances ALP activity, and augments mineral deposition[24].

In the current study, we compared groups treated with β-TCP formulations incorporating individual bio-elements and the control group, revealing markedly elevated ALP activity within the MgO cohort in vitro. Concurrently, the RT-qPCR results showed that mRNA levels of genes encoding *ALP, BMP-2, COL1A1, RUNX2, OC,* and *VEGF*, the indicators of osteoblast differentiation and mineralization, were substantially elevated in the MgO group when compared with those in the control group. Accordingly, these observations suggest the bone-forming tendency of the MgO group.

The capacity of Mg to promote bone formation has been extensively reported. Hou et al. have reported that Mg^{2+} ions can induce osteogenic activity both in vitro and in vivo[25]. Ke et al. have shown that in vitro, MgO-containing β-TCP formulations affect the expression of the osteogenesis-related genes *OPG*, *RANKL*, *BMP-2*, *RUNX2*, and *VEGF*, which influence the process of osteoblast differentiation[9]. Particularly, the role of *VEGF* is noteworthy considering its angiogenic attributes that facilitate capillary network formation, support early-stage osteoblast survival, and promote late-stage angiogenesis, thereby affecting osteoblast differentiation[26]. In addition, *VEGF* contributes to upregulating *BMP-2* expression in endothelial cells and fostering cross-talk between signaling pathways involving endothelial cells and osteoblasts[27]. These previous findings corroborate our current results, affirming the potent bone-forming effects of MgO.

Moreover, in vivo assessments encompassing ALP activity, histological evaluation, and micro-CT analyses showed that the MgO group exhibited superior new bone formation compared to the control group. These results closely resembled the in vitro observations. Micro-CT was used to compare the two groups in terms of the percentage of area that included the artificial bone and the osteogenic area, and no significant difference was found. This is because measuring the area of bone formation alone in this study was challenging, making it difficult to evaluate the amount of bone formation. Thus, these results suggest that the MgO group demonstrated substantial new bone formation in vivo.

The promising results encompassing the improved biological characteristics of MgO-containing β-TCP formulations have been previously reported in short-term in vitro and long-term in vivo studies[28,29]. The findings of our study contribute to the growing body of evidence and enhance our understanding of the influence of elemental incorporation on bone formation. Moreover, the observations of previous reports align with our findings, wherein the MgO group exhibited enhanced bone-forming capacity both in vivo and in vitro when compared to the control group.

Potential mechanisms for bone formation associated with β-TCP containing other biological elements have been previously reported. Different additives may induce differences in the amounts of the α-TCP phase formed after sintering, particularly when MgO is added, which plays an important role in cell–material interactions in vitro and bone formation in vivo, given that relatively less α-TCP phase is formed after sintering[9]. Compared with previous reports, MgO substantially promoted bone formation in the present study, possibly owing to the low amounts of α-TCP phase produced and differences in manufacturing methods. The effects of different manufacturing methods on osteogenesis need to be confirmed in future investigations.

The limitation of this study pertains to the physicochemical evaluation of the material. Since the material is processed from a block with a porosity of approximately 60% to form discs of appropriate size, there may be variations in structural properties such as porosity and pore size distribution among the disc samples produced.

Therefore, it is possible that a small difference in in vitro/in vivo bone formation promotion may have occurred. And it is inferred that the strength is not the same for all artificial bones. It is one of the subjects of future research to make all the artificial bones have the same strength.

It is also possible that there is variation in the amount of MgO added to each disc.

In vivo, unlike in vitro, the concentration of leaked Mg ions may be locally lower due to the influence of in vivo fluid perfusion and other factors. It is important to investigate dose dependence and is a topic for future research.

Conclusions

The findings of the present study indicate that MgO-containing β-TCP formulations promote bone morphological performance both in vitro and in vivo when compared with control β-TCP formulations without any bio-elements. Accordingly, our findings may contribute to improved surgical outcomes and activities of daily living in patients undergoing surgeries requiring artificial bones, such as orthopedic surgeries, for substantial refractory bone loss.

Methods

Preparation of β-TCP discs

We prepared four types of experimental β-TCP discs with 60% porosity, incorporating 1.0 wt.% of either MgO, ZnO, SrO, or SiO_2, as well as bio-element-free (control) β-TCP discs (diameter: 5 mm) (Olympus Terumo Biomaterials Co., Tokyo, Japan). Bio-element-containing β-TCP formulations were synthesized using a mechanochemical method, as described below.

Precisely, $CaCO_3$ and $CaHPO_4{\cdot}2H_2O$ powders were weighed in a 1:2 molar ratio. Next, the materials, including each element (total 1.0 wt% based on oxide weight; 0.6, 0.8, 0.47, and 0.85 wt% of Mg, Zn, Si, and Sr, respectively), were placed together with their powders in a ball mill pot containing pure water at approximately 23 °C, and the pot was rotated for 10 h to mix and mill the materials. The resulting slurry was dried at approximately

80 °C, followed by calcination at 750 °C. Subsequently, a foaming slurry of β-TCP was prepared using a foaming agent, followed by calcination at 1050 °C for 1 h to obtain porous β-TCP discs repleted with the designated elemental additives[30].

BMSC culture and implantation into artificial bone

All animal experimental procedures performed in this study were approved by the Institutional Animal Care and Use Committee (approval No. 13357). This study was conducted in accordance with the National Institutes of Health standards and ARRIVE guidelines (Animal Research: Reporting In Vivo Experiments). Laboratory rats were housed in cages at optimal temperatures below 21 °C under a 12-h light/dark cycle and had ad libitum access to food and water.

Collection and preparation of BMSCs were performed as described previously[12,31,32]. Briefly, 7-week-old male Fisher 344 rats (SLC Japan, Shizuoka, Japan) were placed in sealed containers. General anesthesia was applied using 4% isoflurane (Pfizer, Poor's, Belgium), the bilateral femurs of the rats were removed, and bone marrow was collected.

Subsequently, BMSCs were cultured in 75 cm^2 culture flasks (Falcon; BD Biosciences, San Jose, CA, USA). The minimum essential medium was used (Nacalai Tesque, Kyoto, Japan), to which 15% fetal bovine serum (GE Healthcare Life Sciences, USA) and antibiotics (100 U/mL penicillin and 100 µg/mL streptomycin; Nacalai Tesque, Japan) were added. Approximately 15 mL of medium was used per flask. Cells were incubated at 37 °C in a humidified atmosphere of 95% air and 5% carbon dioxide. Cells not adhering to the flasks were removed at medium changes every three weeks. BMSCs were maintained in primary culture for 14 d. Subsequently, BMSCs were harvested from the confluent medium using trypsin (2.5 g/L) and ethylenediaminetetraacetic acid (EDTA; 1 mmol/L; Nacalai Tesque, Japan).

Next, BMSCs were implanted onto β-TCP discs with 60% porosity containing either MgO, ZnO, SrO, or SiO_2 (experimental) or no bio-elements (control). The β-TCP discs containing MgO, ZnO, SrO, or SiO_2 and control β-TCP discs were placed in a syringe containing a cell solution housing BMSCs with a concentration of 1.0×10^6 cells/cm^2. BMSCs were loaded onto each β-TCP disc by applying negative pressure to the syringe[10,33].

In vitro studies

Each β-TCP disc was placed in a 24-well plate and cultured for 14 days in an osteogenic medium containing 10.0 nmol/L dexamethasone (Sigma, St. Louis, MO, USA), 0.28 mmol/L L-ascorbic acid phosphate magnesium salt n-hydrate (Wako Pure Chemical Industrials, Kyoto, Japan), and 10.0 mmol/L β-glycerol phosphate disodium salt pentahydrate (Nacalai Tesque, Japan). To assess the osteogenic potential of the regimen, Ca concentrations in the supernatant solution were quantified on days 0, 7, and 14. Using reverse transcription-quantitative PCR (RT-qPCR), we then measured the expression of osteogenic markers, i.e., alkaline phosphatase (*ALP*), bone morphogenetic protein 2 (*BMP-2*), collagen type I alpha 1 (*COL1A1*), runt-related transcription factor 2 (*RUNX2*), osteocalcin (*OC*), and vascular endothelial growth factor (*VEGF*), on day 14. In addition, ALP activity was measured on day 14.

Evaluation of Ca concentrations in culture supernatants

The Ca concentrations in culture supernatants were measured on days 7 and 14 using a methyl xylenol blue absorbance spectrophotometric kit (calcium E test; Fujifilm Wako Pure Chemicals, Osaka, Japan), in strict accordance with the manufacturer's instructions. The decrease in Ca contents in the culture medium correspondingly reflected the quantum of Ca deposition onto the artificial bone. Therefore, the Ca concentrations in the culture medium can be used as a marker of tissue-engineered bone formation.

Evaluation of ALP activity

The ALP activity was measured as an important differentiation marker of the osteoblast phenotype to evaluate the osteogenic potential of BMSCs in β-TCP discs. As previously reported, β-TCP constructs were homogenized with 1 mL of 0.2% Nonidet P-40 and centrifuged at 1000×*g* for 10 min at 4 °C. The supernatant (10 µL) was incubated with a buffer containing 56 mmol/L amino-2-methylpropane diol, 10.0 mmol/L *p*-nitrophenyl phosphate, and 1.0 mmol/L $MgCl_2$ at 37 °C for 30 min. The reaction was then stopped by adding 0.2 N NaOH. The ALP activity was estimated by quantifying the absorbance of *p*-nitrophenol at 410 nm using a spectrophotometer (n = 4)[34,35].

RT-qPCR analysis

RT-qPCR was performed as previously reported[12]. Briefly, β-TCP discs were crushed after 14 days of osteogenic culture using 1 mL of TRIzol (Invitrogen; Thermo Fisher Scientific Inc., Waltham, MA, USA) in a micro-homogenizer using purified water at 23 °C. The homogenized β-TCP discs were transferred to a QIA shredder spin column (Qiagen Inc., Valencia, CA, USA) and centrifuged at 17,700×*g* for 2 min before filtration. Subsequently, the samples were mixed thoroughly with 200 µL of chloroform in new 1.5 mL microtubes. The tubes were left for 5 min and then centrifuged at 4 °C for 15 min at 17,700×*g*. The upper layer of the aqueous solution was filtered out into a new 1.5 mL microtube and thoroughly mixed with 70% ethanol. RNA was collected from the samples using RNeasy Micro Kits (Qiagen, Hilden, Germany). The transcription kit with RNase inhibitor (Thermo Fisher Scientific) was used to reverse-transcribe cDNA following the manufacturer's instructions (Applied Biosystems, Foster City, CA, USA). The thermocycling conditions involved the initial activation of TaqMan Fast Universal PCR Master Mix at 95 °C for 20 s, followed by 40 cycles comprising denaturation at 95 °C for 1 s and annealing and extension at 60 °C for 20 s.

The mRNA expression levels of the *ALP*, *BMP-2*, *COL1A1*, *RUNX2*, *OC*, and *VEGF* genes were evaluated using ALP (Rn00564931 m1), BMP-2 (Rn00567818 m1), COL1A1 (Rn01463848 m1), RUNX2 (Rn01512298 m1),

OC (Rn01455285 g1), and VEGF (Rn01511602 m1) assay kits, respectively, (Thermo Fisher Scientific Inc.) and TaqMan® primer and probe sets (Thermo Fisher Scientific Inc.). Target mRNA levels were normalized against glyceraldehyde-3-phosphate dehydrogenase (*GAPDH*, Rn9999916_s1; Thermo Fisher Scientific Inc.) levels as an internal standard (n = 5).

In vivo studies

Subcutaneous implantation of β-TCP discs in Fisher 344 rats

BMSC-bearing β-TCP discs, i.e., MgO-containing β-TCP discs and control β-TCP discs, were implanted in a subcutaneous pocket on the dorsal surface of 7-week-old male Fisher 344 rats[12,33]. The implanted β-TCP discs were harvested after seven weeks and subjected to an ALP activity assay, RT-qPCR (as for in vitro studies), histological examination, immunofluorescence staining and micro-CT.

Assessment of ALP activity

The ALP activity of β-TCP discs harvested after 7 weeks was quantified as described for the in vitro protocol (n = 3).

RT-qPCR analyses

The RT-qPCR analysis of osteogenic markers (*ALP, BMP-2, COL1A1, RUNX2, OC,* and *VEGF*) was conducted at 7 weeks in accordance with the in vitro paradigm (n = 4).

Histological analyses

For histological evaluation, two samples were randomly selected from the MgO and control groups. First, these samples were fixed in a 10% neutral formalin solution (Fujifilm Wako Pure Chemicals). Secondly, they were decalcified in Decalcifying Solution A (Fujifilm Wako Pure Chemicals) for one day. Each sample was embedded in paraffin, and discs were sliced at the center and stained histologically with hematoxylin and eosin.

Immunofluorescence staining

The artificial bone was fixed with a 4% Paraformaldehyde Phosphate Buffer Solution (Fujifilm Wako Pure Chemicals) and then demineralized using a 20% EDTA solution for 5 days. Paraffin blocks were prepared using the standard method. The slide sections were sliced to a thickness of approximately 3 μm.

For collagen I fluorescence staining, the slides were deparaffinized using 3 xylene baths, followed by 3 alcohol baths, and then placed in distilled water. After rinsing with water in 3 TBS baths for 3 min each, the sections were treated with Proteinase K for antigen retrieval at room temperature for 8 min. Following rinsing in 3 TBS baths for 3 min each, non-specific binding was blocked with skim milk at 37 °C for 30 min.

The primary antibody, Anti-Collagen 1, alpha 1 telopeptide primary antibody rabbit polyclonal [Phospho: 322-COLTt], was diluted 1:100 and incubated overnight at 4 °C. After being washed with TBS, the sections were incubated with Alexa Fluor 488 Donkey anti-rabbit IgG [Invitrogen: A21206] at room temperature for 60 min and mounted with SlowFade Gold antifade reagent with DAPI [Invitrogen: S36938]. The reaction was performed at room temperature for 60 min.

Micro-CT analysis

β-TCP discs that were implanted subcutaneously in the backs of rats were fixed in 10% neutral buffered formalin (Wako Pure Chemicals) and then scanned using a CosmoScan FX high-resolution micro-CT instrument (Rigaku Corp., Tokyo, Japan) at a 360° rotation.

As previously reported, the X-ray source was adjusted to a 90 kVp energy and 88 mA intensity, with an isotropic voxel size of 10 μm and an aluminum/copper filter (Al/Cu, 0.5/0.06), resulting in a 512 × 512 pixel image matrix[12]. We evaluated the areas of mineralized bone tissue in each 2 mm thick β-TCP disk in the MgO and Control groups using micro-CT images.

Statistical analyses

All data were subjected to multiple analyses using Welch's t-test, Mann–Whitney U test, and the Tukey–Kramer test in a one-way analysis of variance. Data analyses were performed using SPSS (ver. 28.0; IBM, Japan) software. Values with $P < 0.05$ were considered statistically significant.

Data availability

The datasets used during the present study are available from the corresponding author on reasonable request.

Received: 7 November 2023; Accepted: 19 August 2024
Published online: 25 August 2024

References

1. Kira, T. *et al.* Bone regeneration with osteogenic matrix cell sheet and tricalcium phosphate: An experimental study in sheep. *World J. Orthop.* **8**, 754–760. https://doi.org/10.5312/wjo.v8.i10.754 (2017).
2. Roberts, T. T. & Rosenbaum, A. J. Bone grafts, bone substitutes and orthobiologics: The bridge between basic science and clinical advancements in fracture healing. *Organogenesis* **8**, 114–124. https://doi.org/10.4161/org.23306 (2012).
3. Hashizume, M. & Yamaguchi, M. Stimulatory effect of beta-alanyl-L-histidinato zinc on cell proliferation is dependent on protein synthesis in osteoblastic MC3T3-E1 cells. *Mol. Cell. Biochem.* **122**, 59–64. https://doi.org/10.1007/BF00925737 (1993).

4. Kishi, S. & Yamaguchi, M. Inhibitory effect of zinc compounds on osteoclast-like cell formation in mouse marrow cultures. *Biochem. Pharmacol.* **48**, 1225–1230. https://doi.org/10.1016/0006-2952(94)90160-0 (1994).
5. Moonga, B. S. & Dempster, D. W. Zinc is a potent inhibitor of osteoclastic bone resorption in vitro. *J. Bone Miner. Res.* **10**, 453–457. https://doi.org/10.1002/jbmr.5650100317 (1995).
6. Bandyopadhyay, A., Bernard, S., Xue, W. & Bose, S. Calcium phosphate-based resorbable ceramics: Influence of MgO, ZnO, and SiO_2 dopants. *J. Am. Ceram. Soc.* **89**, 2675–2688. https://doi.org/10.1111/j.1551-2916.2006.01207.x (2006).
7. Silva, D. F., Friis, T. E., Camargo, N. H. A. & Xiao, Y. Characterization of mesoporous calcium phosphates from calcareous marine sediments containing Si, Sr and Zn for bone tissue engineering. *J. Mater. Chem. B* **4**, 6842–6855. https://doi.org/10.1039/c6tb02255c (2016).
8. Mestres, G., Le Van, C. & Ginebra, M.-P. Silicon-stabilized a-tricalcium phosphate and its use in a calcium phosphate cement: Characterization and cell response. *Acta Biomater.* **8**, 1169–1179 (2012).
9. Ke, D., Tarafder, S., Vahabzadeh, S. & Bose, S. Effects of MgO, ZnO, SrO, and SiO_2 in tricalcium phosphate scaffolds on in vitro gene expression and in vivo osteogenesis. *Mater. Sci. Eng. C Mater. Biol. Appl.* **96**, 10–19. https://doi.org/10.1016/j.msec.2018.10.073 (2019).
10. Kawasaki, S. *et al.* In vitro osteogenesis of rat bone marrow mesenchymal cells on PEEK disks with heat-fixed apatite by CO_2 laser bonding. *BMC Musculoskelet. Disord.* **21**, 692. https://doi.org/10.1186/s12891-020-03716-1 (2020).
11. Egawa, T. *et al.* Silicate-substituted strontium apatite nano coating improves osteogenesis around artificial ligament. *BMC Musculoskelet. Disord.* **20**, 396. https://doi.org/10.1186/s12891-019-2777-8 (2019).
12. Sugimoto, H. *et al.* Silicate/zinc-substituted strontium apatite coating improves the osteoinductive properties of beta-tricalcium phosphate bone graft substitute. *BMC Musculoskelet. Disord.* **22**, 673. https://doi.org/10.1186/s12891-021-04563-4 (2021).
13. O'Neill, E., Awale, G., Daneshmandi, L., Umerah, O. & Lo, K. W. H. The roles of ions on bone regeneration. *Drug Discov. Today* **23**, 879–890. https://doi.org/10.1016/j.drudis.2018.01.049 (2018).
14. Gu, X., Zheng, Y., Cheng, Y., Zhong, S. & Xi, T. In vitro corrosion and biocompatibility of binary magnesium alloys. *Biomaterials* **30**, 484–498. https://doi.org/10.1016/j.biomaterials.2008.10.021 (2009).
15. Witte, F. Reprint of: the history of biodegradable magnesium implants: A review. *Acta Biomater.* **23**(Suppl), S28–S40. https://doi.org/10.1016/j.actbio.2015.07.017 (2015).
16. Mayer, I., Schlam, R. & Featherstone, J. D. Magnesium-containing carbonate apatites. *J. Inorg. Biochem.* **66**, 1–6. https://doi.org/10.1016/s0162-0134(96)00145-6 (1997).
17. Wang, S. *et al.* Effect of strontium-containing on the properties of Mg-doped wollastonite bioceramic scaffolds. *Biomed. Eng. OnLine* **18**, 1–14 (2019).
18. Li, X. *et al.* The optimum zinc content in set calcium phosphate cement for promoting bone formation in vivo. *Mater. Sci. Eng. C Mater. Biol. Appl.* **29**, 969–975. https://doi.org/10.1016/j.msec.2008.08.021 (2009).
19. Fielding, G. A., Bandyopadhyay, A. & Bose, S. Effects of silica and zinc oxide doping on mechanical and biological properties of 3D printed tricalcium phosphate tissue engineering scaffolds. *Dent. Mater.* **28**, 113–122. https://doi.org/10.1016/j.dental.2011.09.010 (2012).
20. Wallach, S. Effects of magnesium on skeletal metabolism. *Magnes. Trace Elem.* **9**, 1–14 (1990).
21. Sojka, J. E. & Weaver, C. M. Magnesium supplementation and osteoporosis. *Nutr. Rev.* **53**, 71–74. https://doi.org/10.1111/j.1753-4887.1995.tb01505.x (1995).
22. Salamanca, E. *et al.* Magnesium modified β-tricalcium phosphate induces cell osteogenic differentiation in vitro and bone regeneration in vivo. *Int. J. Mol. Sci.* **23**, 1717. https://doi.org/10.3390/ijms23031717 (2022).
23. Yoshizawa, S., Brown, A., Barchowsky, A. & Sfeir, C. Magnesium ion stimulation of bone marrow stromal cells enhances osteogenic activity, simulating the effect of magnesium alloy degradation. *Acta Biomater.* **10**, 2834–2842. https://doi.org/10.1016/j.actbio.2014.02.002 (2014).
24. Kim, H. K. *et al.* Comprehensive study on the roles of released ions from biodegradable Mg-5 wt% Ca-1 wt% Zn alloy in bone regeneration. *J. Tissue Eng. Regen. Med.* **11**, 2710–2724. https://doi.org/10.1002/term.2166 (2017).
25. Hou, P. *et al.* Magnesium promotes osteogenesis via increasing OPN expression and activating CaM/CaMKIV/CREB1 pathway. *J. Biomed. Mater. Res. B Appl. Biomater.* **110**, 1594–1603. https://doi.org/10.1002/jbm.b.35020 (2022).
26. Tombran-Tink, J. & Barnstable, C. J. Osteoblasts and osteoclasts express PEDF, VEGF-A isoforms, and VEGF receptors: Possible mediators of angiogenesis and matrix remodeling in the bone. *Biochem. Biophys. Res. Commun.* **316**, 573–579. https://doi.org/10.1016/j.bbrc.2004.02.076 (2004).
27. Nakano, K. *et al.* Promotion of osteogenesis and angiogenesis in vascularized tissue-engineered bone using osteogenic matrix cell sheets. *Plast. Reconstr. Surg.* **137**, 1476–1484. https://doi.org/10.1097/PRS.0000000000002079 (2016).
28. Bose, S., Tarafder, S., Banerjee, S. S., Davies, N. M. & Bandyopadhyay, A. Understanding in vivo response and mechanical property variation in MgO, SrO and SiO_2 doped β-TCP. *Bone* **48**, 1282–1290. https://doi.org/10.1016/j.bone.2011.03.685 (2011).
29. Ke, D., Robertson, S. F., Dernell, W. S., Bandyopadhyay, A. & Bose, S. Effects of MgO and SiO_2 on plasma-sprayed hydroxyapatite coating: An in vivo study in rat distal femoral defects. *ACS Appl. Mater. Interfaces* **9**, 25731–25737. https://doi.org/10.1021/acsami.7b05574 (2017).
30. Kakuta, A. *et al.* Effects of micro-porosity and local BMP-2 administration on bioresorption of beta-TCP and new bone formation. *Biomater. Res.* **23**, 12. https://doi.org/10.1186/s40824-019-0161-2 (2019).
31. Akahane, M. *et al.* Scaffold-free cell sheet injection results in bone formation. *J. Tissue Eng. Regen. Med.* **4**, 404–411. https://doi.org/10.1002/term.259 (2010).
32. Nakamura, A. *et al.* Cell sheet transplantation of cultured mesenchymal stem cells enhances bone formation in a rat nonunion model. *Bone* **46**, 418–424. https://doi.org/10.1016/j.bone.2009.08.048 (2010).
33. Akahane, M. *et al.* Osteogenic matrix sheet-cell transplantation using osteoblastic cell sheet resulted in bone formation without scaffold at an ectopic site. *J. Tissue Eng. Regen. Med.* **2**, 196–201. https://doi.org/10.1002/term.81 (2008).
34. Inagaki, Y. *et al.* Osteogenic matrix cell sheet transplantation enhances early tendon graft to bone tunnel healing in rabbits. *Biomed. Res. Int.* **2013**, 842192. https://doi.org/10.1155/2013/842192 (2013).
35. Ueha, T. *et al.* Utility of tricalcium phosphate and osteogenic matrix cell sheet constructs for bone defect reconstruction. *World J. Stem Cells* **7**, 873–882. https://doi.org/10.4252/wjsc.v7.i5.873 (2015).

Acknowledgements

The authors would like to thank Ms. Fumika Kunda (Nara Medical University Faculty of Medicine, Japan) for her technical assistance. We would also like to thank Editage (www.editage.com) for English language editing.

Author contributions

K.S. and Y.I. contributed to the overall design and conduct of the study, analysis of the results, and preparation of the manuscript. Y.U., M.O., A.K., and Y.T. contributed to the overall design and management of the study. K.O., M.O., Y.N. and A.K. contributed to the conduct of the experiments and analysis of the results. T.S. contributed to the development of the artificial bone. All authors read and approved the final submitted manuscript.

Competing interests
This research was funded by Olympus Terumo Biomaterials Corp.

Additional information
Correspondence and requests for materials should be addressed to Y.I.